



Adipocyte mTORC1 deficiency promotes adipose tissue inflammation and NLRP3 inflammasome activation via oxidative stress and de novo ceramide synthesis^S

Patricia Chimin,^{1,*†} Maynara L. Andrade,^{1,*} Thiago Belchior,* Vivian A. Paschoal,* Juliana Magdalon,* Alex S. Yamashita,* Ériquer Castro,* Angela Castoldi,[§] Adriano B. Chaves-Filho,** Marcos Y. Yoshinaga,** Sayuri Miyamoto,** Niels O. Câmara,[§] and William T. Festuccia^{2,*}

Departments of Physiology and Biophysics* and Immunology,[§] Institute of Biomedical Sciences, and Department of Biochemistry,** Institute of Chemistry, University of Sao Paulo, Sao Paulo, Brazil 05508000; and Department of Physical Education,[†] Physical Education and Sports Center, Londrina State University, Parana, Brazil 86051-990

Abstract Mechanistic target of rapamycin complex (mTORC)1 activity is increased in adipose tissue of obese insulin-resistant mice, but its role in the regulation of tissue inflammation is unknown. Herein, we investigated the effects of adipocyte mTORC1 deficiency on adipose tissue inflammation and glucose homeostasis. For this, mice with adipocyte raptor deletion and controls fed a chow or a high-fat diet were evaluated for body mass, adiposity, glucose homeostasis, and adipose tissue inflammation. Despite reducing adiposity, adipocyte mTORC1 deficiency promoted hepatic steatosis, insulin resistance, and adipose tissue inflammation (increased infiltration of macrophages, neutrophils, and B lymphocytes; crown-like structure density; TNF- α , interleukin (IL)-6, and monocyte chemoattractant protein 1 expression; IL-1 β protein content; lipid peroxidation; and de novo ceramide synthesis). The anti-oxidant, N-acetylcysteine, partially attenuated, whereas treatment with de novo ceramide synthesis inhibitor, myriocin, completely blocked adipose tissue inflammation and nucleotide oligomerization domain-like receptor pyrin domain-containing 3 (NLRP3)-inflammasome activation, but not hepatic steatosis and insulin resistance induced by adipocyte raptor deletion. Rosiglitazone treatment, however, completely abrogated insulin resistance induced by adipocyte raptor deletion. **In conclusion, adipocyte mTORC1 deficiency induces adipose tissue inflammation and NLRP3-inflammasome activation by promoting oxidative stress and de novo ceramide synthesis. Such adipose tissue inflammation, however, is not an underlying cause of the insulin resistance displayed by these mice.**—Chimin, P., M. L. Andrade, T. Belchior, V. A. Paschoal, J. Magdalon, A. S. Yamashita, É. Castro, A. Castoldi, A. B. Chaves-Filho, M. Y. Yoshinaga,

S. Miyamoto, N. O. Câmara, and W. T. Festuccia. **Adipocyte mTORC1 deficiency promotes adipose tissue inflammation and NLRP3 inflammasome activation via oxidative stress and de novo ceramide synthesis.** *J. Lipid Res.* 2017. 58: 1797–1807.

Supplementary key words mechanistic target of rapamycin complex 1 • nucleotide oligomerization domain-like receptor pyrin domain-containing 3 • insulin resistance

Chronic low-intensity inflammation is an important linking factor between visceral obesity and associated metabolic complications such as insulin resistance (1). Mechanistically, obesity-associated inflammation is triggered through the activation of the canonical toll-like receptor (TLR)4-I κ B kinase (IKK)-nuclear factor kappa-light-chain-enhancer of activated

Abbreviations: ASC/PyCARD, apoptosis-associated speck-like protein containing a CARD; CASP1, caspase 1; CAT, catalase; CLS, crown-like structure; DEPTOR, DEP domain containing mechanistic target of rapamycin-interacting protein; DUSP6, dual specificity phosphatase 6; FACS, fluorescence-activated cell sorting; G6Pase, glucose 6-phosphatase; GPx, glutathione peroxidase; GTT, glucose tolerance test; HFD, high-fat diet; IKK, I κ B kinase; IL, interleukin; IIT, insulin tolerance test; LPS, lipopolysaccharide; MCP, monocyte chemoattractant protein; MDA, malondialdehyde; mTOR, mechanistic target of rapamycin; mTORC, mechanistic target of rapamycin complex; MYR, myriocin; NAC, N-acetylcysteine; NF κ B, nuclear factor kappa-light-chain-enhancer of activated B cells; NLRP3, nucleotide oligomerization domain-like receptor pyrin domain-containing 3; PEPCK, phosphoenolpyruvate carboxykinase; PI3K, phosphoinositide 3 kinase; PyCARD, PYD and CARD domain containing; RapKO, raptor^{Lox/Lox} adiponectin-cre^{+/-} mice; RicKO, rictor^{Lox/Lox} adiponectin-cre^{+/-} mice; RapWT, raptor^{Lox/Lox} adiponectin-cre^{-/-} mice; RicKO, rictor^{Lox/Lox} adiponectin-cre^{+/-} mice; RicWT, rictor^{Lox/Lox} adiponectin-cre^{-/-}; ROS, reactive oxygen species; RSG, rosiglitazone; S6, p70 ribosomal S6 kinase; SCD1, stearoyl-CoA saturase 1; SMPD, SM phosphodiesterase; SOD, superoxide dismutase; SPTLC, serine palmitoyltransferase long chain base; TLR, toll-like receptor; UCP1, uncoupling protein 1.

¹ P. Chimin and M. L. Andrade contributed equally to this work.

² To whom correspondence should be addressed.

e-mail: william.festuccia@gmail.com

^S The online version of this article (available at <http://www.jlr.org>) contains a supplement.

This work was supported by Fundação de Amparo à Pesquisa do Estado de São Paulo Grants 09/15354-7, 10/52191-6, and 15/19530-5 (to W.T.F.) and 12/02270-2 (to N.O.C.) and Conselho Nacional de Desenvolvimento Científico e Tecnológico Grants 454226/2014-4 (to P.C.) and 443492/2014-0 (to W.T.F.). Additional support was provided by Fundação de Amparo à Pesquisa do Estado de São Paulo Fellowships 12/25317-4 and 15/13508-8 (to P.C. and M.L.A., respectively). The authors do not have any potential conflicts of interest relevant to this article.

Manuscript received 22 December 2016 and in revised form 13 June 2017.

Published, JLR Papers in Press, July 5, 2017

DOI <https://doi.org/10.1194/jlr.M074518>

Copyright © 2017 by the American Society for Biochemistry and Molecular Biology, Inc.

This article is available online at <http://www.jlr.org>

B cells (NF κ B) signaling by the gram-negative bacterial wall component lipopolysaccharide (LPS) from gut microbiota and/or excessive amounts of saturated fatty acids (2–4).

One important proinflammatory event triggered by TLR4-IKK-NF κ B signaling upon obesity is the activation of nucleotide oligomerization domain-like receptor pyrin domain-containing 3 (NLRP3)-inflammasome, a multimeric cytosolic protein complex activated by pathogen- and danger-associated molecular patterns, that promotes caspase 1 (CASP1)-mediated interleukin (IL)-1 β processing and secretion (5). Mechanistically, NLRP3-inflammasome activation by TLR4-IKK-NF κ B requires a priming step characterized by an increase in NLRP3 and pro-IL-1 β mRNA and protein contents followed by an activation step defined by inflammasome protein complex assembly (5, 6). Mitochondrial reactive oxygen species (ROS), saturated fatty acids, and cholesterol crystals, among others, were shown to induce inflammasome priming, whereas ceramides, potassium efflux, and mitochondrial DNA induce inflammasome assembly and activation (6).

Obesity, through unknown mechanisms, is also associated with a chronic activation of mechanistic target of rapamycin complex (mTORC)1 in adipose tissue (7). mTORC1, which is composed of mammalian lethal with Sec13 protein 8 (mLST8), Tti1/Tel2 complex, DEP domain-containing mTOR-interacting protein (DEPTOR), regulatory-associated protein of mTOR (raptor), proline-rich Akt substrate 40 kDa (PRAS40), and the serine/threonine kinase mTOR as its catalytic center, is mainly activated by amino acids and growth factors and regulates protein and lipid syntheses, autophagy, and adipose tissue mass and metabolism (8). Specifically regarding the regulation of adiposity, recent findings obtained from mice with adipocyte mTORC1 constitutive activation [tuberous sclerosis 1 (Tsc1) deletion] (9) or deficiency (raptor deletion) (10, 11) or mild inhibition (DEPTOR overexpression) (12) indicate that optimal levels of mTORC1 activity, neither too high nor too low, are required for its pro-fat accretion actions (9). Interestingly, in spite of markedly reducing adiposity, adipocyte raptor deletion (mTORC1 deficiency) using either ap2- or adiponectin-cre has resulted in different glucose homeostasis outcomes. Indeed, while ap2-cre-driven raptor deletion protected mice from diet-induced obesity, glucose intolerance, and insulin resistance, promoted adipose tissue browning, and increased energy expenditure (10), adiponectin-cre-driven raptor deletion induced hepatic steatosis and insulin resistance, as evidenced by fasting hyperinsulinemia and impaired insulin tolerance (11).

Changes in adiposity are generally associated with alterations in adipose tissue-resident leukocyte content and profile. Indeed, obesity is characterized by enhanced macrophage recruitment and polarization to a proinflammatory M1 profile (1), while the opposite, i.e., caloric restriction, reduces adipose tissue mass and macrophage infiltration and induces leukocyte polarization to a M2 anti-inflammatory profile (13). In addition to growth factors and amino acids, mTORC1 is also activated by proinflammatory molecules, such as LPS and cytokines, via TLR4 signaling through either IKK (14) or phosphoinositide 3 kinase (PI3K)-mTOR

complex 2 (mTORC2)-Akt (15, 16), as well as by anti-inflammatory IL-4 and IL-13 (14), being therefore an important regulator of innate and adaptive immune responses (17). In spite of its activation in “inflamed” fat in obesity, little is known about the role of mTORC1 in the regulation of adipose tissue inflammation. Indeed, pharmacological mTOR inhibition with rapamycin was shown to exacerbate obesity-associated adipose tissue inflammation by increasing tissue infiltration of proinflammatory M1 macrophages, as well as content of TNF- α , IL-6, and monocyte chemoattractant protein (MCP)1 (18, 19). Because of the systemic nature of rapamycin, partial inhibitory activity toward mTORC1, and off-target to mTORC2 (8), it was impossible in these studies to delineate the contribution of adipocyte mTOR complexes in the regulation of adipose tissue inflammation. Therefore, we investigated, herein, the effects of adipocyte-specific raptor (mTORC1 deficiency) and rictor (mTORC2 deficiency) deletions on adipose tissue inflammation and glucose homeostasis in mice fed with a chow or high-fat diet (HFD).

METHODS

Mice and treatments

Animal experimental procedures were approved by the Animal Care Committee of the Institute of Biomedical Sciences, University of Sao Paulo, Brazil (098/2010 and 093/2012, CEUA). Mice were obtained from the Jackson Laboratory (Bar Harbor, ME) on a C57BL6/J background and kept at 22 \pm 1°C, 12:12 h light-dark cycle, with free access to tap water and food ad libitum. Adipocyte raptor or rictor deletion was produced by crossing raptor^{Lox/Lox} (B6.Cg-Rptor^{tm1.1Dmsa/J}) and rictor^{Lox/Lox} (rictor^{tm1.1Klg/3jml}) mice with adiponectin-cre mice [B6;FVB-Tg(Adipoq-cre)1Evdrr/J]. Heterozygous raptor^{Lox/WT};adiponectin-cre and rictor^{Lox/WT};adiponectin-cre offspring were then crossed with raptor^{Lox/Lox} and rictor^{Lox/Lox} mice to obtain raptor^{Lox/Lox};adiponectin-cre and rictor^{Lox/Lox};adiponectin-cre (henceforth referred to as RapKO and RicKO, respectively) and their littermates raptor^{Lox/Lox} and rictor^{Lox/Lox} (henceforth referred to as RapWT and RicWT, respectively) mice. Mice were fed with a standard chow diet (NUVILAB CR-1-Sogorb Inc., São Paulo, Brazil; 63% carbohydrates, 25% protein, and 12% fat; percent kilocalories) or a HFD (20% carbohydrates, 20% protein, 60% fat; percent kilocalories) for 8 weeks and evaluated for body weight and food intake weekly. After 8 weeks, 6 h-fasted mice were euthanized for tissue and blood harvesting. Cohorts of chow-fed RapWT and RapKO mice were treated with either vehicle or the antioxidant, N-acetylcysteine (NAC; 300 mg/kg; Sigma) or the antibiotic and serine palmitoyltransferase long chain (SPTLC) inhibitor, myriocin (MYR; 0.5 mg/kg; Sigma) once daily by gavage during 7 days. Doses of NAC and MYR were previously described (20, 21). A cohort of HFD-fed RapWT and RapKO mice was also treated with the PPAR γ agonist, rosiglitazone (RSG; 30 mg/kg/day), as an admixture in the diet for 8 weeks (22).

Serum insulin, glucose, and insulin tolerance tests

Serum insulin was measured by ELISA following supplier recommendations (Millipore, Billerica, MA). Glucose tolerance tests (GTTs) and insulin tolerance tests (ITTs) were performed in 6 h-fasted mice injected intraperitoneally with either glucose (1 g/kg) or insulin (0.75 U/kg), respectively. Tail-vein blood glycemia was determined before and 15, 30, 45, 60, and 90 min

after glucose injection or 5, 10, 15, 20, and 30 min after insulin injection using a OneTouch Johnson & Johnson glucometer. Plasma glucose disappearance rate (kITT, percent per minute) in the ITT was calculated as before (22).

Isolation of mature adipocytes and stromal-vascular fraction

Epididymal adipose tissue was digested with collagenase type II (1 mg/ml; Sigma-Aldrich) in Krebs-HEPES buffer containing BSA (1%) and glucose (2 mmol/l), pH 7.4 at 37°C. After filtering, the cell suspension was centrifuged (600 g, 10 min) for isolation of floating mature adipocytes and stromal-vascular cells (pellet) for PCR and flow cytometry analysis.

Flow cytometry analysis

Stromal-vascular cells (2×10^6 cells) were incubated with red blood cell lysis buffer (5 min), centrifuged, resuspended in Fc block, and analyzed for leukocyte content in a FACSCanto II, essentially as previously described (18). Ten thousand events per sample were acquired with a Diva-Software™ and analyzed with FlowJo 10.0.7. Antibodies used in fluorescence-activated cell sorting (FACS) analysis are detailed in supplemental Table S1.

RNA extraction and quantitative real-time PCR

Adipose tissue, mature adipocytes, and stromal-vascular cell total RNA were extracted with Trizol (Invitrogen Life Technologies), reverse transcribed to cDNA, and evaluated by quantitative real-time PCR using a Rotor Gene (Qiagen) and SYBR Green as fluorescent dye, as previously described (16). Data are expressed as the ratio of target and reference genes (36B4 and HPRT1), which were not significantly affected by raptor or rictor deletion. Primer sequences are detailed on supplemental Table S2.

Western blotting

Protein extracts from epididymal fat pad were resolved on polyacrylamide gels, transferred to PVDF membranes, blocked with 5% milk, and incubated with primary and secondary antibodies, as previously described (9). Primary antibodies are detailed in supplemental Table S3. Membranes were developed using the ECL substrate (GE Healthcare Life Sciences). Densitometric analyses were performed with ImageJ (National Institutes of Health).

Histological analysis

Epididymal adipose tissue was fixed in 4% formaldehyde and embedded in paraffin, cross-sectioned (5 μ m), deparaffinized, and stained with hematoxylin-eosin. Crown-like structures (CLSs) were identified as single adipocytes surrounded by macrophages, counted along with total adipocyte number, and expressed as number per 1,000 adipocytes, essentially as previously described (23).

Malondialdehyde content

Adipose tissue malondialdehyde (MDA) content was measured with a reversed-phase HPLC (Agilent Technologies 1200 series; Santa Clara, CA) after thiobarbituric acid derivatization, as described (24). Fluorometric detection at excitation and emission wavelengths of 515 and 543 nm, respectively, was used to quantify MDA using a standard regression prepared with 1,1,3,3-tetraethoxypropane (0.5–15.0 μ M).

Catalase activity

Catalase (CAT) activity was measured as previously described (25). Briefly, 30 mg of tissue were homogenized in 50 mM phosphate buffer and centrifuged at 6,000 g for 10 min. The supernatant was incubated with 30 mM hydrogen peroxide for about 30 s at 20°C. The absorbance was set at 240 nm.

ELISA

Protein extracts from epididymal adipose tissue, prepared as previously described (9), were evaluated for IL-1 β content by ELISA (eBioscience, San Diego, CA), following the manufacturer's recommendations.

Adipose tissue glucose uptake, fatty acid profile, and ceramide content

Adipose tissue insulin-stimulated glucose uptake and fatty acid profile were evaluated essentially as previously described (9, 26). For ceramide quantification, briefly, adipose tissue was homogenized in 10 mM sodium phosphate buffer (pH 7.4) containing 100 μ M deferoxamine mesylate and the internal standard, *N*-heptadecanoyl-D-erythro-sphingosylphosphorylcholine (SM d18:1/17:0). Lipids were extracted with methyl-tert-butyl ether/methanol. The organic phase containing lipids was dried under nitrogen stream, suspended in isopropanol, and analyzed in an ultra (U)HPLC (Nexera; Shimadzu, Kyoto, Japan) coupled to an electrospray ionization TOF mass spectrometer (Triple TOF 6600; Sciex, Framingham, MA). Lipids were separated on a UPLC reversed-phase column (CORTECS® C18 column, 1.6 μ m, 2.1 mm internal diameter \times 100 mm). Lipid molecular species were identified with an in-house Excel-based macro based on the MS and MS/MS fragmentation pattern observed with PeakView®. Quantification was performed with MultiQuant®, where peak areas of precursor ions were normalized to those of the internal standards.

Statistical analysis

Differences between genotypes, treatments, and their combination were evaluated by Student's unpaired *t*-tests or multifactorial ANOVA followed by Newman-Keuls test, when appropriate. Data were assessed for sphericity using Mauchly's test, and whenever the test was violated, technical correction through the Greenhouse-Geisser test was performed. The statistical level of significance was set at $P < 0.05$. Data were analyzed using Graph Prism® (GraphPad Software Inc., San Diego, CA). Results are presented as mean \pm SEM.

RESULTS

We have previously shown that pharmacological mTORC1 inhibition with rapamycin exacerbates obesity-associated glucose intolerance and adipose tissue inflammation (18). In an attempt to investigate whether adipocyte mTORC1 deficiency would mimic the exacerbation of fat tissue inflammation induced by rapamycin, mice with raptor deletion exclusively in adipocytes (RapKO) and littermate controls (RapWT) were fed with a chow diet or HFD for 8 weeks and evaluated for several parameters. As depicted in **Fig. 1A**, RapKO mice had reduced adipose tissue protein content of raptor, total and phosphorylated (p)S6 and 4E binding protein, and increased pSer473Akt, confirming the impairment in mTORC1 activity induced by raptor deletion. Confirming previous studies (10, 11), RapKO mice fed with a chow diet had reduced body weight gain and masses of retroperitoneal and epididymal fat depots and were completely protected from the increase in adiposity induced by HFD intake (**Fig. 1B–D**). This reduced adiposity was associated with a reduction in adipocyte diameter and mRNA levels of important lipogenic enzymes, CD36, LPL, and FABP4 (supplemental **Fig. S1A–C**). It is noteworthy that HFD feeding increased body weight gain in RapKO

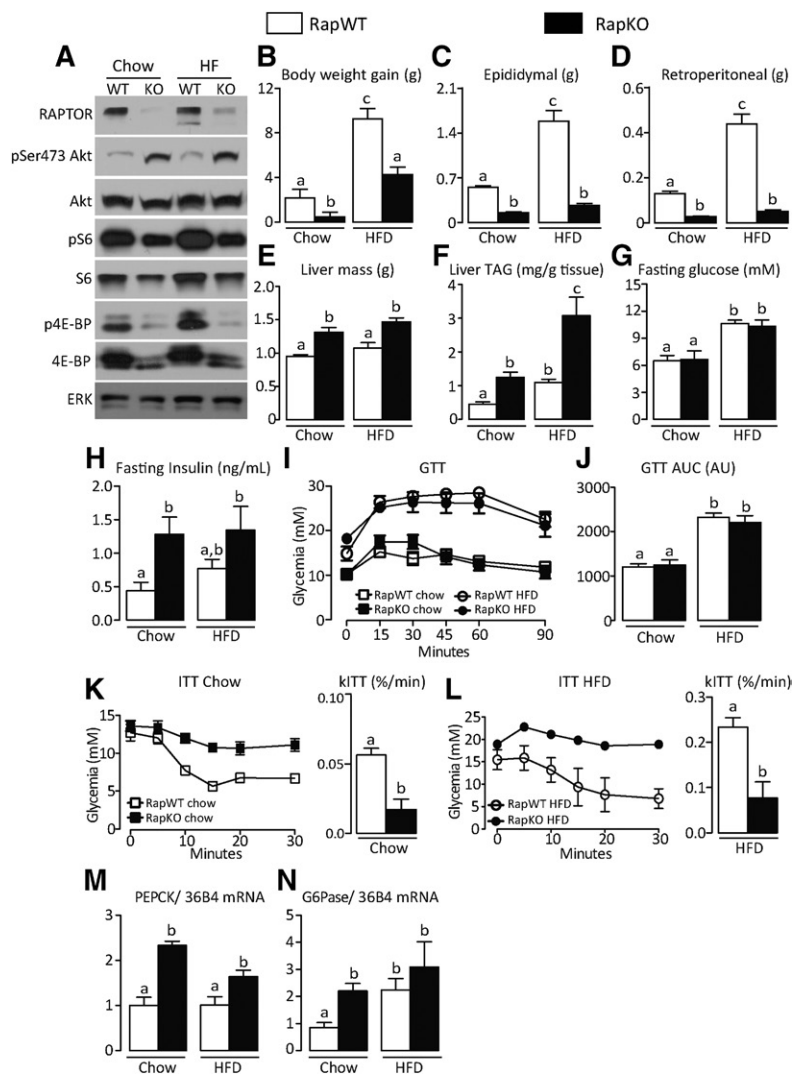


Fig. 1. Adipocyte raptor deletion reduces adiposity and promotes hepatic steatosis and insulin resistance in mice. Adipose tissue mTORC1 and mTORC2 signaling (A); body weight gain (B); epididymal (C), retroperitoneal (D), and liver mass (E); liver triacylglycerol (TAG) content (F); fasting glucose (G), and insulin (H); GTT (I), and area under the curve (AUC) (J); ITT and rates of glucose disappearance (kITT) (K, L); and liver mRNA levels of PEPCK (M) and G6Pase (N) in RapWT and RapKO mice fed with chow or HFD for 8 weeks. Values are mean \pm SEM of 6–12 mice. Means not sharing a common superscript are significantly different from each other, $P < 0.05$.

mice, which seemed to be due to exacerbated hepatic lipid accumulation (Fig. 1E, F) as the result of the inability of adipose tissue to store lipids. Along with hepatic steatosis and independently of diet, RapKO mice were insulin resistant, as evidenced by the higher fasting hyperinsulinemia, insulin intolerance, and liver mRNA levels of the gluconeogenic enzymes, phosphoenolpyruvate carboxykinase (PEPCK) and glucose 6-phosphatase (G6Pase) (Fig. 1H, K–N). No changes, however, were seen in fasting glycemia or glucose tolerance between RapKO and RapWT mice (Fig. 1G, I, J).

Interestingly, despite the reduced body weight and adiposity, adipocyte mTORC1 deficiency induced adipose tissue inflammation in chow-fed mice, as evidenced by the increased percentage of resident M1 (F4/80⁺ CD11b⁺ CD86⁺) and M2 (F4/80⁺ CD11b⁺ CD206⁺) macrophages, neutrophils (Ly6G⁺) and B lymphocytes (CD19⁺), CLS density, and mRNA levels of the macrophage markers, F4/80 (total), CD86 (M1), and CD206 (M2), and the cytokines, MCP1, IL-6, and TNF- α (Fig. 2A–H). The adipose tissue percentage of dendritic cells and T lymphocytes was not altered by raptor deletion (data not shown). In addition, adipocyte mTORC1 deficiency significantly increased adipose

tissue mRNA levels of inflammasome components, NLRP3, apoptosis-associated speck-like protein containing a CARD (ASC/PyCARD), and IL-1 β , and protein content of pro-IL-1 β and IL-1 β in chow-fed mice (Fig. 2H–J). Interestingly, raptor deletion promoted inflammasome activation in adipocytes, but not in stromal vascular cells, as evidenced by the increased mRNA levels of NLRP3, DUSP-6, and IL-1 β exclusively in adipocytes (supplemental Fig. S1D, E). Of note, similarly to raptor deletion, chronic rapamycin treatment significantly increased adipose tissue mRNA levels of the inflammasome components, NLRP3, ASC/PyCARD, DUSP-6, and IL-1 β in HFD-fed mice without affecting body weight gain or adiposity (data not shown). Altogether, these findings indicate that adipocyte mTORC1 deficiency, despite reducing adipose tissue mass and independently of diet, promotes adipose tissue inflammation and adipocyte NLRP3-inflammasome activation.

We next investigated to determine whether adipocyte deficiency of mTORC2, an upstream regulator of mTORC1 activity that is also activated by LPS and other proinflammatory factors through the TLR4-PI3K pathway (15, 16), promotes adipose tissue inflammation. As depicted in supplemental Fig. S2A, adipocyte rictor deletion effectively

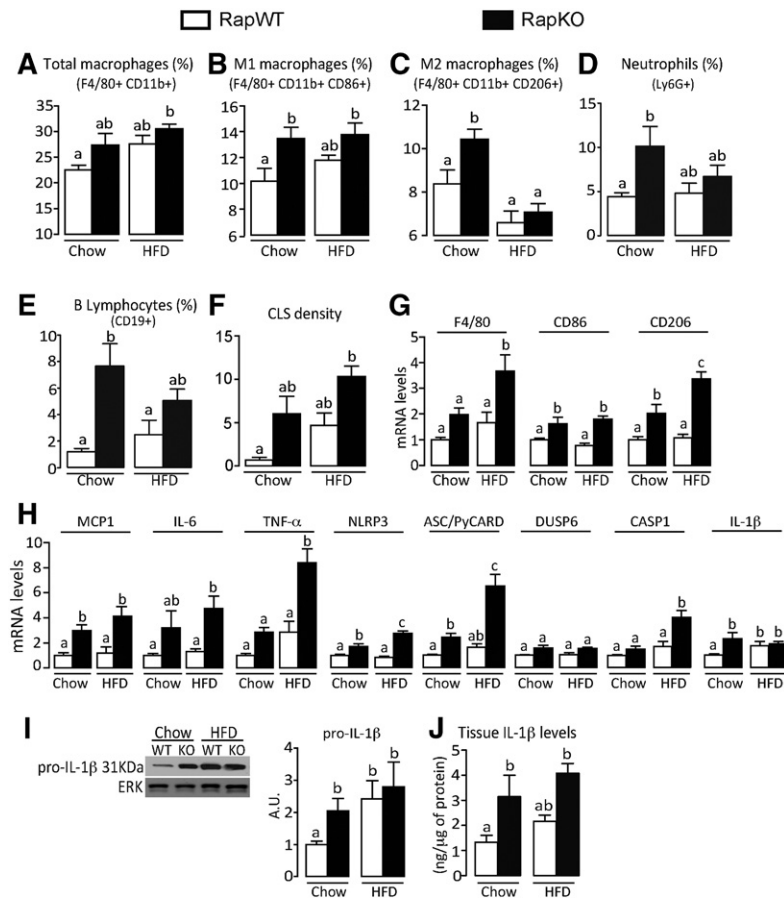


Fig. 2. Adipocyte raptor deletion induces adipose tissue inflammation and NLRP3-inflammasome activation. Adipose tissue-resident total (A) (F4/80⁺,CD11b⁺), M1 (B) (F4/80⁺,CD11b⁺,CD86⁺,CD206⁻), and M2 (C) (F4/80⁺,CD11b⁺,CD206⁺,CD86⁻) macrophages, neutrophils (D) (Ly6G⁺), and B lymphocytes (E) (CD19⁺); CLS density (F); mRNA levels of macrophage markers (G); cytokines and NLRP3-inflammasome components (H); pro-IL-1β (I) (Western); and IL-1β tissue content (J) (ELISA) in RapWT and RapKO mice fed with chow or HFD for 8 weeks. Values are mean ± SEM of 6–12 mice. Means not sharing a common superscript are significantly different from each other, *P* < 0.05.

attenuated mTORC2 activity, as evidenced by the reduced adipose tissue content of pSer473 and total Akt. In contrast to mTORC1, mTORC2 deficiency did not affect body weight gain and adiposity in chow-fed mice (supplemental Fig. S2B–D). Upon intake of HFD, however, RicKO mice displayed reduced epididymal and retroperitoneal masses, but no major changes in body weight gain when compared with HFD-fed RicWT mice. Extensive analysis of the adipose tissue leukocyte profile by either FACS (data not shown) or PCR did not reveal any significant changes between RicKO and RicWT mice independently of the diet (supplemental Fig. S2E–G). No changes between genotypes were seen in adipose tissue mRNA levels of cytokines, with the exception of IL-6, which was significantly increased in chow-fed RicKO mice (supplemental Fig. S2F). Altogether, these findings indicate that adipocyte mTORC2 deficiency reduces fat mass, but in contrast to mTORC1 deficiency, it does not promote adipose tissue inflammation.

In an attempt to elucidate the mechanisms underlying NLRP3-inflammasome activation in RapKO mice, we next investigated in chow-fed mice whether adipocyte raptor deficiency was associated with changes in tissue oxidative stress and ceramides, important activators of NLRP3-inflammasome. As illustrated in Fig. 3A, adipocyte raptor deletion significantly increased adipose tissue mRNA levels of superoxide dismutase (SOD)2, a mitochondrial enzyme that catalyzed the conversion of superoxide into hydrogen peroxide and molecular oxygen, but reduced those of CAT and glutathione peroxidase (GPx)1, both

enzymes that catalyze the reduction of hydrogen peroxide to water. Extending those findings, adipocyte raptor deletion increased adipose tissue mRNA and protein content of mitochondrial uncoupling protein 1 (UCP1), reduced CAT activity, and increased tissue content of MDAs, a secondary product of lipid hydroperoxide decomposition and marker of lipid peroxidation (Fig. 3A–E). It is noteworthy that, along with oxidative stress, adipocyte raptor deletion altered the adipose tissue fatty acid profile by elevating the percentage of saturated palmitic (16:0) and stearic acids (18:0) and reducing the percentage of mono-unsaturated palmitoleic (16:1, n-7) and oleic acids (18:1, n-9) (Fig. 3F–I). Accordingly, protein content of stearoyl-CoA desaturase 1 (SCD1), which catalyzes the conversion of saturated fatty acids into monounsaturated fatty acids, was significantly reduced in adipose tissue of RapKO mice (Fig. 3E). Because tissue accumulation of saturated fatty acids is generally associated with increased ceramide synthesis, we next investigated the expression of several genes involved in this process. As depicted in Fig. 3J, adipocyte raptor deletion markedly increased adipose tissue mRNA levels of SPTLC-1, SPTLC-2, and SPTLC-3, enzymes that are rate-limiting in the de novo pathway of ceramide synthesis. No changes, however, were seen in mRNA levels of SM phosphodiesterase (SMPD)-1 and SMPD-2, enzymes that produce ceramide from the hydrolysis of membrane SM. These findings indicate that adipocyte mTORC1 deficiency induces adipose tissue oxidative stress and increases de novo ceramide synthesis.

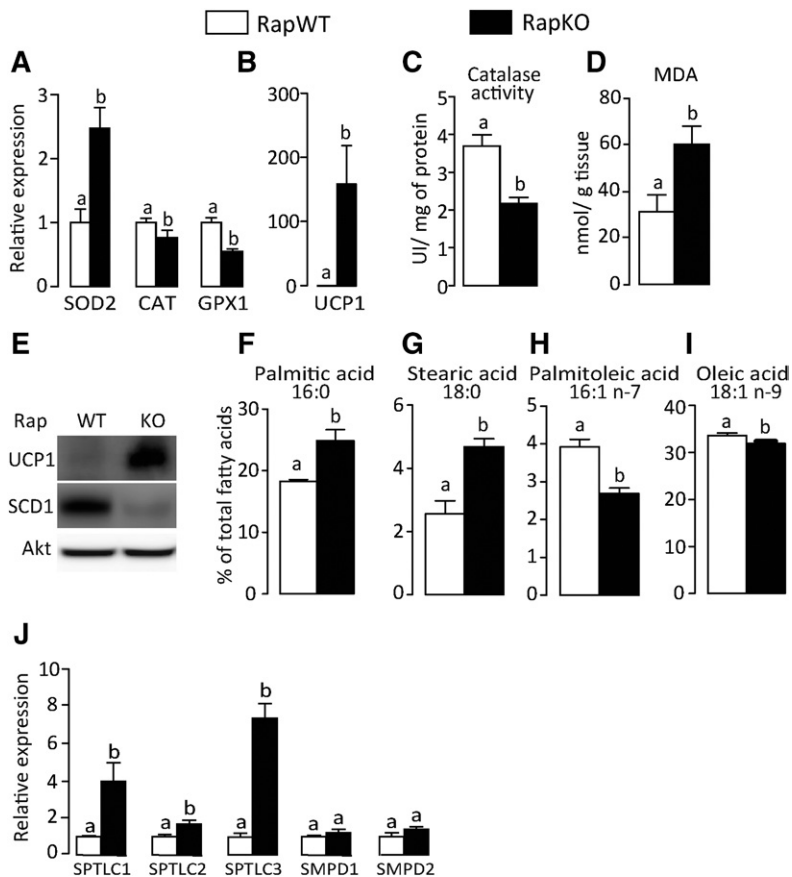


Fig. 3. Adipocyte raptor deletion induces adipose tissue oxidative stress and ceramide production. Adipose tissue mRNA levels of oxidative stress markers (A) and UCP1 (B); CAT activity (C); MDA content (D); protein content of mitochondrial UCP1 and SCD1 (E); percentage of palmitic (F), stearic (G), palmitoleic (H), and oleic (I) acids; and mRNA levels of enzymes involved in the ceramide synthesis (J) in chow-fed RapWT and RapKO mice. Values are mean \pm SEM of four to eight mice. Means not sharing a common superscript are significantly different from each other, $P < 0.05$.

To test the involvement of oxidative stress in adipose tissue inflammation and NLRP3-inflammasome activation induced by adipocyte mTORC1 deficiency, we treated chow-fed RapKO and RapWT mice with the antioxidant agent, NAC, for 7 days by gavage. Although NAC did not affect body weight, adiposity, and liver mass in both RapKO and RapWT mice (supplemental Fig. 3A–E), it attenuated adipose tissue oxidative stress in RapKO mice, as evidenced by the restoration of SOD2, CAT, and GPx1 mRNA levels to levels found in RapWT mice (Fig. 4A). Surprisingly, NAC attenuated the increase in adipose tissue mRNA levels and protein content of UCP1 induced by raptor deletion (Fig. 4B, C). In addition to oxidative stress, NAC also attenuated RapKO fat tissue inflammation, as evidenced by the reduction in adipose tissue mRNA levels of macrophage markers, F4/80, CD86, and CD206, and the density of CLSs (Fig. 4D, E). Furthermore, NAC completely abrogated the increase in adipose tissue mRNA levels of a few components of NLRP3-inflammasome induced by raptor deficiency, namely NLRP3, dual specificity phosphatase 6 (DUSP6), and CASP1, but surprisingly, it did not affect the high mRNA levels of ASC/PyCARD and further increased those of IL-1 β (Fig. 4F). Extending those findings, NAC did not affect adipose tissue protein content of pro-IL-1 β and IL-1 β , as evaluated by both ELISA and Western blotting (Fig. 4G–I). Altogether these findings indicate that oxidative stress is partially involved in the induction of adipose tissue UCP1 expression, inflammation, and NLRP3-inflammasome activation induced by mTORC1 deficiency in adipocytes.

Because oxidative stress only partially explained the changes in adipose tissue promoted by adipocyte raptor deletion, we next investigated whether ceramides could act as mediators of those phenotypes. For this, we treated another cohort of RapWT and RapKO mice for 7 days with the SPTLC inhibitor, MYR, which blocks de novo ceramide synthesis. MYR did not affect body weight gain, adipose tissue mass, and protein contents of Akt pSer473 and UCP1 or adipocyte area in both RapWT and RapKO mice (supplemental Fig. S4F–J and Fig. 5F). As depicted in Fig. 5A–C, however, MYR completely abrogated the increases in adipose tissue content of the ceramide d18:1/16:0, mRNA levels of macrophage markers F4/80, CD86, and CD206, and density of CLS induced by raptor deletion. Furthermore, MYR completely blocked NLRP3-inflammasome activation induced by adipocyte mTORC1 deficiency, as evidenced by the restoration to levels found in controls of NLRP3, ASC/PyCARD, and IL-1 β mRNA levels and pro-IL-1 β and IL-1 β protein content evaluated by both ELISA and Western blotting (Fig. 5D–F). Along with the abrogation of adipose tissue inflammation, MYR restored insulin-stimulated glucose uptake in adipose tissue to levels of controls without affecting, however, insulin intolerance and fasting hyperinsulinemia displayed by RapKO mice (Fig. 5G–J). Altogether, these findings indicate that adipocyte mTORC1 deficiency promotes adipose tissue inflammation and NLRP3-inflammasome activation by inducing de novo ceramide synthesis, and that such inflammatory process does not seem to be an underlying cause of the insulin intolerance featured by RapKO mice.

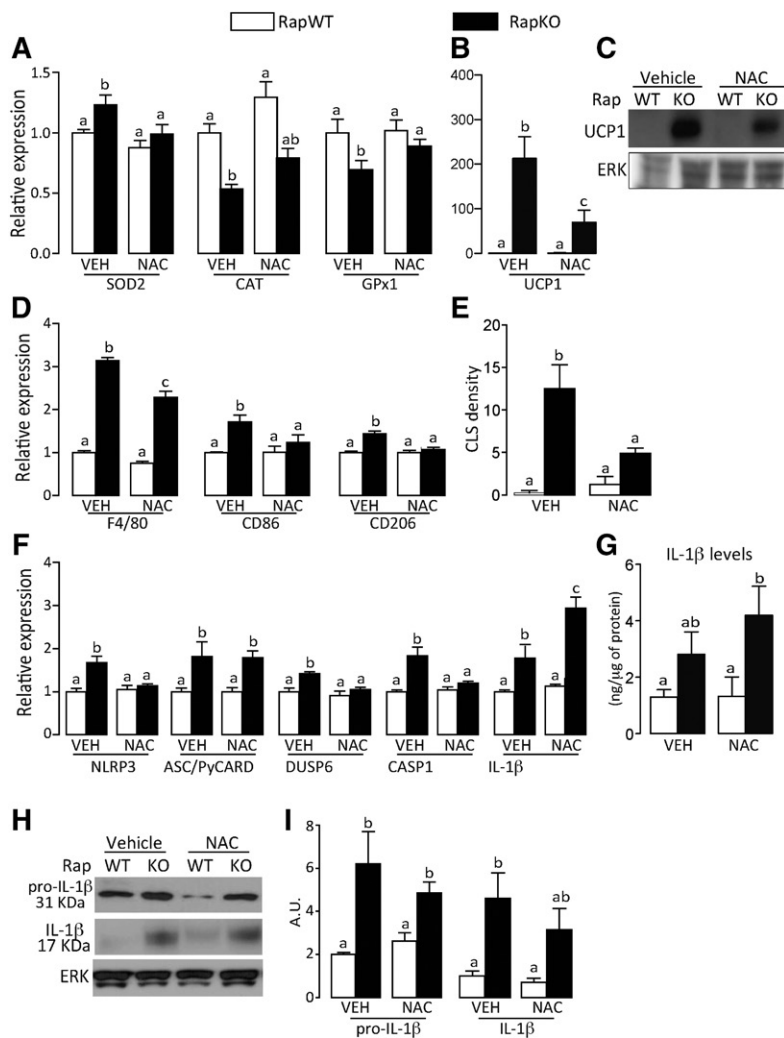


Fig. 4. NAC attenuates adipose tissue inflammation induced by adipocyte raptor deletion. Adipose tissue mRNA levels of oxidative stress markers (A) and UCP1 (B); protein content of UCP1 (C); mRNA levels of macrophage markers (D); CLS density (E); mRNA levels of NLRP3-inflammasome components (F); IL-1 β content (G) (ELISA); and pro-IL-1 β and mature IL-1 β protein contents (H, I) (Western) in chow-fed RapWT and RapKO mice treated with vehicle (VEH) or NAC (300 mg/kg) by gavage for 7 days. Values are mean \pm SEM of four to eight mice. Means not sharing a common superscript are significantly different from each other, $P < 0.05$.

In the face of our previous findings that pharmacological PPAR γ activation attenuates the glucose intolerance induced by rapamycin in rats (22), we next tested to determine whether RSG was effective in improving glucose homeostasis in HFD-fed RapKO mice. As illustrated in the **Fig. 6A–D**, 8 weeks of RSG treatment did not affect body weight gain or liver mass in RapWT and RapKO mice. Confirming previous findings, RSG induced only a reduction in visceral adiposity in RapWT mice, as evidenced by the reduced masses of epididymal and retroperitoneal adipose depots (Fig. 6B, C). RSG improved glucose homeostasis in RapKO mice, as evidenced by complete abrogation of insulin intolerance, elevated liver PEPCK mRNA levels, and fasting hyperinsulinemia featured by these mice (Fig. 6E–H). Surprisingly, along with glucose homeostasis, RSG only partly attenuated adipose tissue inflammation in RapKO mice, as evidenced by the reduction in mRNA levels of the inflammasome components, NLRP3, DUSP6, and IL-1 β , but not of MCP1 and CD86, a marker of activated macrophages (Fig. 6I).

DISCUSSION

We investigated herein whether adipocyte mTORC1 and mTORC2 deficiencies modulate adipose tissue inflammation

and glucose homeostasis. Independently of diet and despite reducing adiposity, adipocyte mTORC1, but not mTORC2, deficiency promotes insulin intolerance, hepatic steatosis, and an inflammatory process in adipose tissue characterized by enhanced percentage of resident M1 and M2 macrophages, neutrophils, and B lymphocytes, increased density of CLSs, elevated expression of proinflammatory cytokines/chemokines (TNF- α , IL-6, and MCP1), and activation of NLRP3-inflammasome-mediated IL-1 β production. Mechanistically, such adipose tissue inflammation and NLRP3-inflammasome activation, which resulted from enhanced oxidative stress and de novo ceramide synthesis, do not seem to be an underlying cause of insulin resistance featured by RapKO mice.

Confirming a previous study, adipocyte mTORC1 deficiency markedly reduced adipose tissue mass and protected from HFD-induced obesity, but induced, independently of diet, hepatic steatosis and insulin resistance, as evidenced by the enhanced liver triacylglycerol content, fasting hyperinsulinemia, and insulin intolerance. Mechanistically, hepatic steatosis is likely the result of a liver lipid overload due to the reduced ability of adipose tissue to store fatty acids (11, 27). Indeed, raptor deletion in adipocytes markedly reduced adipose tissue mRNA levels of important pro-lipid storage proteins, LPLs, and fatty acid transporters, CD36

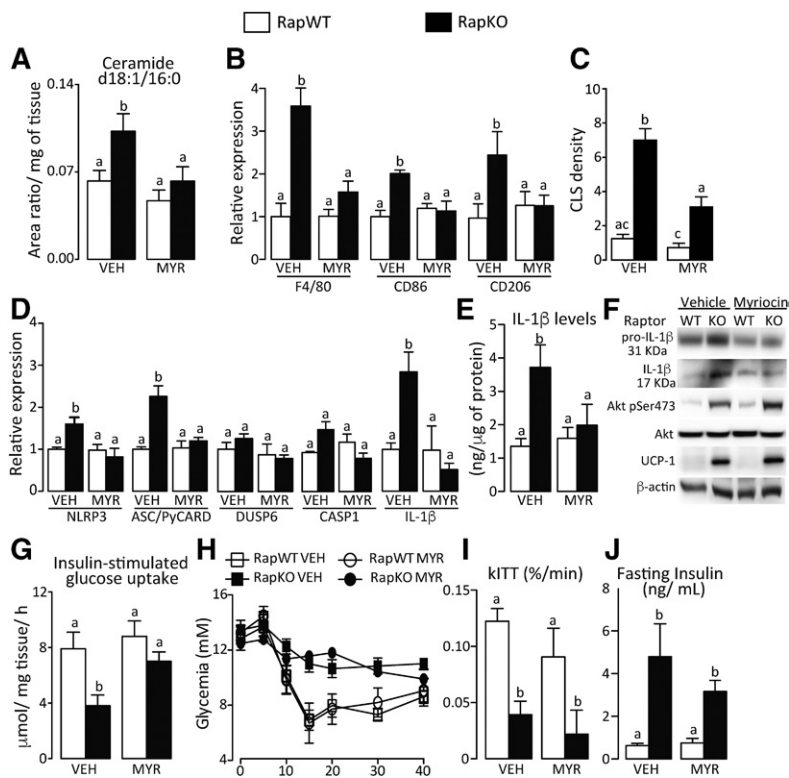


Fig. 5. MYR abrogated adipose tissue inflammation and inflammasome activation induced by adipocyte raptor deletion. Adipose tissue content of ceramide d18:1/16:0 (A); mRNA levels of macrophage markers (B); CLS density (C); mRNA levels of NLRP3-inflammasome components (D); IL-1 β content (E) (ELISA); and pro-IL-1 β and mature IL-1 β , Akt, and UCP1 contents (F) (Western); adipose tissue insulin-stimulated glucose uptake (G); ITT (H); and rates of glucose disappearance (kITT) (I) and fasting insulinemia (J) in chow-fed RapWT and RapKO mice treated with vehicle (VEH) or MYR (0.5 mg/kg) by gavage for 7 days. Values are mean \pm SEM of four to eight mice. Means not sharing a common superscript are significantly different from each other, $P < 0.05$.

and FABP4. Regarding insulin intolerance, our findings that liver PEPCK and G6Pase mRNA levels are increased in RapKO mice indicate a likely involvement of gluconeogenesis as an underlying cause. Indeed, elevated fatty acid flux to liver and oxidation has been shown to increase gluconeogenic flux through a mechanism that involves allosteric activation of pyruvate carboxylase by acetyl-CoA generated by fatty acid β oxidation (28).

We showed herein that the reduction in adiposity induced by adipocyte raptor deletion is associated with adipose tissue inflammatory process characterized by increased macrophage, neutrophil, and B lymphocyte recruitment, CLS density, expression of proinflammatory cytokines, and NLRP3-inflammasome activity. Importantly, with exception of neutrophils, those inflammatory phenotypes were also seen in adipose tissue upon chronic treatment of HFD-fed mice with rapamycin, as shown here and before (18), indicating that adipocyte mTORC1 may be central to the adipose tissue inflammation induced by systemic pharmacological mTORC1 inhibition. Besides those similarities, raptor deletion promotes inflammation independently of diet, while rapamycin induces inflammation only in HFD-fed mice and without majorly affecting adiposity. These discrepancies may relate to the fact that rapamycin, in contrast to raptor deletion, only partially inhibits mTORC1 (8). Differences aside, our findings that genetic and pharmacological mTORC1 inhibition promotes adipose tissue inflammation suggest that the increased complex activity seen in adipose tissue of obese mice may be a mechanism to avoid excessive tissue inflammation.

In contrast to raptor, adipocyte deletion of rictor, an essential component of mTORC2, does not promote adipose tissue inflammation, in spite of also reducing adiposity.

These findings are in contrast to the inflammatory phenotypes seen upon rictor and raptor deletion in macrophages. Indeed, rictor deletion in macrophages exacerbated the proinflammatory response, polarization to M1 phenotype, and secretion of proinflammatory cytokines by these cells (16); whereas, macrophage raptor deletion is anti-inflammatory (29). These results support the concept that mTORC1 and mTORC2 regulation of inflammation is cell-type specific, as it has been shown for different types of lymphocytes and other leukocytes (17).

One important aspect of the inflammatory process induced by adipocyte raptor deletion is the activation of NLRP3-inflammasome, a phenotype that seems to occur specifically in adipocytes, as evidenced by the absence of changes in the mRNA levels of inflammasome components in stromal-vascular cells of RapKO mice. NOD receptors, such as NLRP3, recognize danger-associated molecular patterns derived from injured cells and tissues, such as ROS, fatty acids, and lipid mediators, among others, promoting, through a series of events, CASP1-mediated IL-1 β cleavage and secretion (30). Because mTORC1 is an important regulator of mitochondrial function and metabolism (31–34), an organelle that is a major source of cellular ROS, we raised the hypothesis that raptor deletion might promote adipose tissue inflammation and NLRP3-inflammasome activation by inducing ROS and oxidative stress. Indeed, previous studies have demonstrated that enhanced mitochondrial ROS production achieved through complex I inhibition promotes an inflammatory process characterized by activation of NF κ B and NLRP3-inflammasome-mediated IL-1 β production (35, 36). Although adipocyte raptor deletion induced oxidative stress in adipose tissue, as evidenced by the reduction in GPx1 mRNA levels and

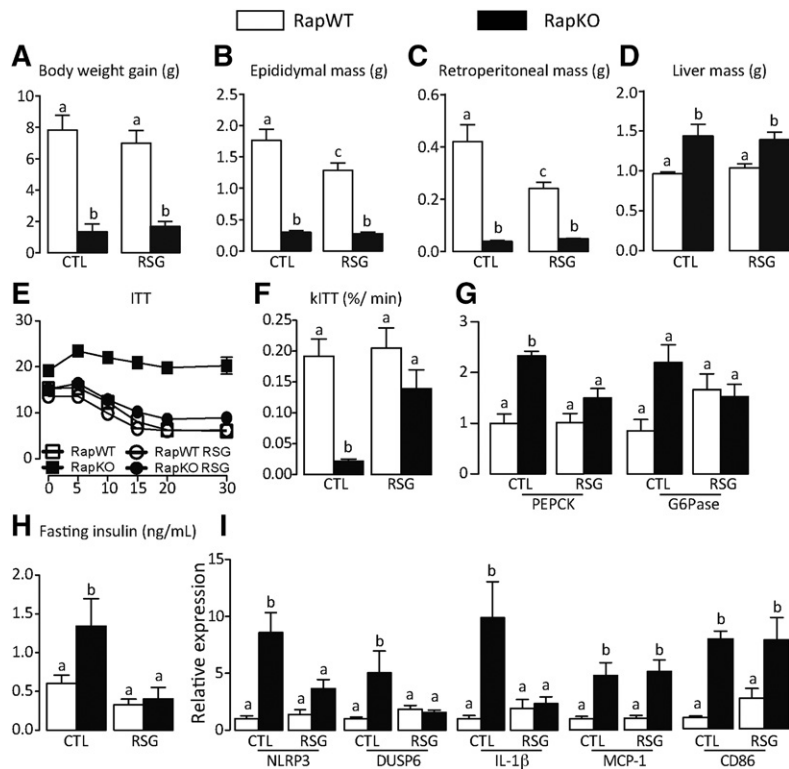


Fig. 6. RSG abrogated insulin resistance induced by adipocyte raptor deletion. Body weight gain (A); epididymal (B), retroperitoneal (C), and liver (D) masses; ITT (E); and rates of glucose disappearance (kITT) (F); liver PEPCK and G6Pase mRNA levels (G); fasting insulin (H); and adipose tissue mRNA levels of inflammatory proteins (I) in HFD-fed RapWT and RapKO mice treated with RSG (30 mg/kg/day) as admixture in the diet for 8 weeks. Values are mean \pm SEM of four to eight mice. Means not sharing a common superscript are significantly different from each other, $P < 0.05$.


CAT activity and enhanced lipid peroxidation, treatment with antioxidant NAC only partially attenuated some of the inflammatory markers investigated (CLS density and mRNA levels of macrophage markers and few inflammasome components). Of special interest, NAC did not affect adipose tissue NLRP3-inflammasome activity, as evidenced by the absence of changes in pro-IL-1 β and IL-1 β protein content. Altogether, these findings indicate that, in mice bearing raptor deletion in adipocytes, oxidative stress is only partially involved in adipose tissue inflammation and primes the NLRP3-inflammasome for further activation. Interestingly, NAC partially blocked the increase in adipose tissue UCP1 content induced by raptor deletion, indicating that UCP1-mediated mitochondrial uncoupling may perhaps be induced to counteract the enhanced mitochondrial ROS production and oxidative stress found upon adipocyte mTORC1 deficiency. It is noteworthy that UCP1 has been shown to attenuate mitochondrial ROS production in situations of enhanced fatty acid oxidation, such as cold exposure (37, 38). Despite reducing adipose tissue UCP1 content, NAC treatment did not affect the reduction in adipose tissue mass induced by raptor deletion, indicating that nonshivering thermogenesis is not a major underlying cause of this phenotype.

Because ceramides have been shown to be important activators of NLRP3-inflammasome (5), we hypothesized that these lipids could be involved in the induction of adipose tissue inflammation by adipocyte raptor deletion. Accordingly, adipocyte raptor deletion increased adipose tissue prevalence of saturated over monounsaturated fatty acids, such fatty acids that are precursors and activators, through TLR4 signaling, of de novo ceramide synthesis (39). This change in adipose tissue fatty acid profile that probably

resulted from reduced SCD1 activity, was also associated with a marked increase in adipose tissue mRNA levels of SPTLC1, SPTLC2, and SPTLC3, rate-limiting enzymes of de novo ceramide synthesis, and content of the ceramide (d18:1/16:0). Finally, pharmacological inhibition of de novo ceramide synthesis with MYR completely abolished adipose tissue inflammation and NLRP3-inflammasome activation induced by raptor deletion, establishing ceramides as major mediators of this phenotype. Interestingly, ceramide has also been reported to induce ROS generation through the inhibition of mitochondrial electron transport chain in several cell types (40, 41), suggesting that both ROS and ceramides could act together in the induction of adipose tissue inflammation and in the priming and activation of NLRP3-inflammasome seen upon adipocyte raptor deletion.

Importantly, despite completely abolishing adipose tissue inflammation and reestablishing adipose tissue insulin-stimulated glucose uptake to control values, MYR did not affect hepatic steatosis and insulin resistance in RapKO mice, as evidenced by the preserved insulin intolerance and fasting hyperinsulinemia in these mice. These findings support the notion that adipose tissue inflammation and impaired insulin-stimulated glucose uptake are not major underlying causes of the insulin resistance induced by adipocyte raptor deletion. Interestingly, RapKO mice displayed impaired adipose tissue insulin-stimulated glucose uptake, despite having a higher content of pAkt Ser473, indicating that the resistance node probably lies downstream to Akt in the activation and translocation of glucose transporter 4 (GLUT4). Administration of the PPAR γ ligand, RSG, to RapKO mice, on the other hand, completely restored insulin tolerance and fasting insulin to levels of controls, without affecting body weight, adipose

tissue mass, and hepatic steatosis. It is noteworthy that RSG was also shown to improve glucose homeostasis in rapamycin-treated rats (22), although, as herein, the mechanisms underlying those actions are still elusive.

In conclusion, our findings indicate that the reduction in adiposity induced by adipocyte mTORC1 deficiency is associated with adipose tissue inflammation and activation of NLRP3-inflammasome-mediated IL-1 β production as a result of tissue oxidative stress and elevated de novo ceramide production. Such adipose tissue inflammatory process, however, does not seem to be an underlying cause of the insulin resistance featured by mice with raptor deletion in adipocytes. Altogether, our findings reinforce the importance of mTORC1 in the regulation of adiposity, inflammation, and adipose tissue fat storage and their intricate relationship with glucose homeostasis. 

The authors would like to thank Thayna Vieira (Institute of Biomedical Sciences, University of Sao Paulo, Brazil) and Luciene Lauer (Faculty of Pharmaceutical Sciences, University of Sao Paulo) for the invaluable technical assistance.

REFERENCES

- Hotamisligil, G. S. 2006. Inflammation and metabolic disorders. *Nature*. **444**: 860–867.
- Bourlier, V., A. Zakaroff-Girard, A. Miranville, S. De Barros, M. Maumus, C. Sengenès, J. Galitzky, M. Lafontan, F. Karpe, K. N. Frayn, et al. 2008. Remodeling phenotype of human subcutaneous adipose tissue macrophages. *Circulation*. **117**: 806–815.
- Henegar, C., J. Tordjman, V. Achard, D. Lacasa, I. Cremer, M. Guerre-Millo, C. Poitou, A. Basdevant, V. Stich, N. Viguèrie, et al. 2008. Adipose tissue transcriptomic signature highlights the pathological relevance of extracellular matrix in human obesity. *Genome Biol*. **9**: R14.
- Hotamisligil, G. S., and E. Erbay. 2008. Nutrient sensing and inflammation in metabolic diseases. *Nat. Rev. Immunol.* **8**: 923–934.
- Vandanmagsar, B., Y. H. Youm, A. Ravussin, J. E. Galgani, K. Stadler, R. L. Mynatt, E. Ravussin, J. M. Stephens, and V. D. Dixit. 2011. The NLRP3 inflammasome instigates obesity-induced inflammation and insulin resistance. *Nat. Med.* **17**: 179–188.
- Henaoui-Mejia, J., E. Elinav, C. A. Thaiss, and R. A. Flavell. 2014. Inflammasomes and metabolic disease. *Annu. Rev. Physiol.* **76**: 57–78.
- Um, S. H., F. Frigerio, M. Watanabe, F. Picard, M. Joaquin, M. Sticker, S. Fumagalli, P. R. Allegrini, S. C. Kozma, J. Auwerx, et al. 2004. Absence of S6K1 protects against age- and diet-induced obesity while enhancing insulin sensitivity. *Nature*. **431**: 200–205.
- Laplante, M., and D. M. Sabatini. 2012. mTOR signaling in growth control and disease. *Cell*. **149**: 274–293.
- Magdalon, J., P. Chimin, T. Belchior, R. X. Neves, M. A. Vieira-Lara, M. L. Andrade, T. S. Farias, A. Bolsoni-Lopes, V. A. Paschoal, A. S. Yamashita, et al. 2016. Constitutive adipocyte mTORC1 activation enhances mitochondrial activity and reduces visceral adiposity in mice. *Biochim. Biophys. Acta*. **1861**: 430–438.
- Polak, P., N. Cybulski, J. N. Feige, J. Auwerx, M. A. Ruegg, and M. N. Hall. 2008. Adipose-specific knockout of raptor results in lean mice with enhanced mitochondrial respiration. *Cell Metab.* **8**: 399–410.
- Lee, P. L., Y. Tang, H. Li, and D. A. Guertin. 2016. Raptor/mTORC1 loss in adipocytes causes progressive lipodystrophy and fatty liver disease. *Mol. Metab.* **5**: 422–432.
- Laplante, M., S. Horvat, W. T. Festuccia, K. Birsoy, Z. Prevorsek, A. Efeyan, and D. M. Sabatini. 2012. DEPTOR cell-autonomously promotes adipogenesis, and its expression is associated with obesity. *Cell Metab.* **16**: 202–212.
- Morris, D. L., K. Singer, and C. N. Lumeng. 2011. Adipose tissue macrophages: phenotypic plasticity and diversity in lean and obese states. *Curr. Opin. Clin. Nutr. Metab. Care*. **14**: 341–346.
- Lee, D. F., H. P. Kuo, C. T. Chen, J. M. Hsu, C. K. Chou, Y. Wei, H. L. Sun, L. Y. Li, B. Ping, W. C. Huang, et al. 2007. IKK beta suppression of TSC1 links inflammation and tumor angiogenesis via the mTOR pathway. *Cell*. **130**: 440–455.
- Martin, M., R. E. Schifferle, N. Cuesta, S. N. Vogel, J. Katz, and S. M. Michalek. 2003. Role of the phosphatidylinositol 3 kinase-Akt pathway in the regulation of IL-10 and IL-12 by *Porphyromonas gingivalis* lipopolysaccharide. *J. Immunol.* **171**: 717–725.
- Festuccia, W. T., P. Pouliot, I. Bakan, D. M. Sabatini, and M. Laplante. 2014. Myeloid-specific Rictor deletion induces M1 macrophage polarization and potentiates in vivo pro-inflammatory response to lipopolysaccharide. *PLoS One*. **9**: e95432.
- Weichhart, T., M. Hengstschläger, and M. Linke. 2015. Regulation of innate immune cell function by mTOR. *Nat. Rev. Immunol.* **15**: 599–614.
- Paschoal, V. A., M. T. Amano, T. Belchior, J. Magdalon, P. Chimin, M. L. Andrade, M. Ortiz-Silva, E. Castro, A. S. Yamashita, J. C. Rosa Neto, et al. 2017. mTORC1 inhibition with rapamycin exacerbates adipose tissue inflammation in obese mice and dissociates macrophage phenotype from function. *Immunobiology*. **222**: 261–271.
- Makki, K., S. Taront, O. Molendi-Coste, E. Bouchaert, B. Neve, E. Eury, S. Lobbens, M. Labalette, H. Duez, B. Staels, et al. 2014. Beneficial metabolic effects of rapamycin are associated with enhanced regulatory cells in diet-induced obese mice. *PLoS One*. **9**: e92684.
- Ivanovski, O., D. Szumilak, T. Nguyen-Khoa, N. Ruellan, O. Phan, B. Lacour, B. Descamps-Latscha, T. B. Drüeke, and Z. A. Massy. 2005. The antioxidant N-acetylcysteine prevents accelerated atherosclerosis in uremic apolipoprotein E knockout mice. *Kidney Int.* **67**: 2288–2294.
- Ussher, J. R., T. R. Koves, V. J. Cadete, L. Zhang, J. S. Jaswal, S. J. Swyrd, D. G. Lopaschuk, S. D. Proctor, W. Keung, D. M. Muoio, et al. 2010. Inhibition of de novo ceramide synthesis reverses diet-induced insulin resistance and enhances whole-body oxygen consumption. *Diabetes*. **59**: 2453–2464.
- Festuccia, W. T., P. G. Blanchard, T. Belchior, P. Chimin, V. A. Paschoal, J. Magdalon, S. M. Hirabara, D. Simões, P. St-Pierre, A. Carpinelli, et al. 2014. PPAR γ activation attenuates glucose intolerance induced by mTOR inhibition with rapamycin in rats. *Am. J. Physiol. Endocrinol. Metab.* **306**: E1046–E1054.
- Murano, I., G. Barbatelli, V. Parisani, C. Latini, G. Muzzonigro, M. Castellucci, and S. Cinti. 2008. Dead adipocytes, detected as crown-like structures, are prevalent in visceral fat depots of genetically obese mice. *J. Lipid Res.* **49**: 1562–1568.
- Hong, Y. L., S. L. Yeh, C. Y. Chang, and M. L. Hu. 2000. Total plasma malondialdehyde levels in 16 Taiwanese college students determined by various thiobarbituric acid tests and an improved high-performance liquid chromatography-based method. *Clin. Biochem.* **33**: 619–625.
- Aebi, H. 1984. Catalase in vitro. *Methods Enzymol.* **105**: 121–126.
- Belchior, T., V. A. Paschoal, J. Magdalon, P. Chimin, T. M. Farias, A. B. Chaves-Filho, R. Gorjão, P. St-Pierre, S. Miyamoto, J. X. Kang, et al. 2015. Omega-3 fatty acids protect from diet-induced obesity, glucose intolerance, and adipose tissue inflammation through PPAR γ -dependent and PPAR γ -independent actions. *Mol. Nutr. Food Res.* **59**: 957–967.
- Cortés, V. A., D. E. Curtis, S. Sukumaran, X. Shao, V. Parameswara, S. Rashid, A. R. Smith, J. Ren, V. Esser, R. E. Hammer, et al. 2009. Molecular mechanisms of hepatic steatosis and insulin resistance in the AGPAT2-deficient mouse model of congenital generalized lipodystrophy. *Cell Metab.* **9**: 165–176.
- Perry, R. J., J. P. Camporez, R. Kursawe, P. M. Titchenell, D. Zhang, C. J. Perry, M. J. Jurczak, A. Abudukadier, M. S. Han, X. M. Zhang, et al. 2015. Hepatic acetyl CoA links adipose tissue inflammation to hepatic insulin resistance and type 2 diabetes. *Cell*. **160**: 745–758.
- Jiang, H., M. Westerterp, C. Wang, Y. Zhu, and D. Ai. 2014. Macrophage mTORC1 disruption reduces inflammation and insulin resistance in obese mice. *Diabetologia*. **57**: 2393–2404.
- Lukens, J. R., V. D. Dixit, and T. D. Kanneganti. 2011. Inflammasome activation in obesity-related inflammatory diseases and autoimmunity. *Discov. Med.* **12**: 65–74.
- Cunningham, J. T., J. T. Rodgers, D. H. Arlow, F. Vazquez, V. K. Mootha, and P. Puigserver. 2007. mTOR controls mitochondrial oxidative function through a YY1-PGC-1 α transcriptional complex. *Nature*. **450**: 736–740.
- Deepa, S. S., M. E. Walsh, R. T. Hamilton, D. Pulliam, Y. Shi, S. Hill, Y. Li, and H. Van Remmen. 2013. Rapamycin modulates markers

- of mitochondrial biogenesis and fatty acid oxidation in the adipose tissue of db/db mice. *J. Biochem. Pharmacol. Res.* **1**: 114–123.
33. Morita, M., S. P. Gravel, V. Chénard, K. Sikström, L. Zheng, T. Alain, V. Gandin, D. Avizonis, M. Arguello, C. Zakaria, et al. 2013. mTORC1 controls mitochondrial activity and biogenesis through 4E-BP-dependent translational regulation. *Cell Metab.* **18**: 698–711.
34. Schieke, S. M., D. Phillips, J. P. McCoy, A. M. Aponte, R. F. Shen, R. S. Balaban, and T. Finkel. 2006. The mammalian target of rapamycin (mTOR) pathway regulates mitochondrial oxygen consumption and oxidative capacity. *J. Biol. Chem.* **281**: 27643–27652.
35. Tschopp, J., and K. Schroder. 2010. NLRP3 inflammasome activation: the convergence of multiple signalling pathways on ROS production? *Nat. Rev. Immunol.* **10**: 210–215.
36. Harijith, A., D. L. Ebenezer, and V. Natarajan. 2014. Reactive oxygen species at the crossroads of inflammasome and inflammation. *Front. Physiol.* **5**: 352.
37. Brand, M. D., C. Affourtit, T. C. Esteves, K. Green, A. J. Lambert, S. Miwa, J. L. Pakay, and N. Parker. 2004. Mitochondrial superoxide: production, biological effects, and activation of uncoupling proteins. *Free Radic. Biol. Med.* **37**: 755–767.
38. Oelkrug, R., M. Kutschke, C. W. Meyer, G. Heldmaier, and M. Jastroch. 2010. Uncoupling protein 1 decreases superoxide production in brown adipose tissue mitochondria. *J. Biol. Chem.* **285**: 21961–21968.
39. Holland, W. L., B. T. Bikman, L. P. Wang, G. Yuguang, K. M. Sargent, S. Bulchand, T. A. Knotts, G. Shui, D. J. Clegg, M. R. Wenk, et al. 2011. Lipid-induced insulin resistance mediated by the pro-inflammatory receptor TLR4 requires saturated fatty acid-induced ceramide biosynthesis in mice. *J. Clin. Invest.* **121**: 1858–1870.
40. García-Ruiz, C., A. Colell, M. Marí, A. Morales, and J. C. Fernández-Checa. 1997. Direct effect of ceramide on the mitochondrial electron transport chain leads to generation of reactive oxygen species. Role of mitochondrial glutathione. *J. Biol. Chem.* **272**: 11369–11377.
41. Park, J. Y., M. J. Kim, Y. K. Kim, and J. S. Woo. 2011. Ceramide induces apoptosis via caspase-dependent and caspase-independent pathways in mesenchymal stem cells derived from human adipose tissue. *Arch. Toxicol.* **85**: 1057–1065.